NASA TN D-918

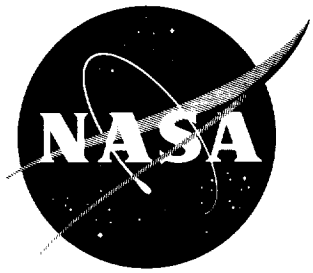

# TECHNICAL NOTE

D-918

## TRANSONIC WIND-TUNNEL INVESTIGATION OF THE FIN LOADS ON A 1/8-SCALE MODEL SIMULATING THE FIRST STAGE OF THE SCOUT RESEARCH VEHICLE

By Thomas C. Kelly

Langley Research Center
Langley Field, Va.

NATIONAL AERONAUTICS AND SPACE ADMINISTRATION

WASHINGTON

June 1961

lW

NATIONAL AERONAUTICS AND SPACE ADMINISTRATION

TECHNICAL NOTE D-918

# TRANSONIC WIND-TUNNEL INVESTIGATION OF THE FIN LOADS ON A 1/8-SCALE MODEL SIMULATING THE FIRST STAGE OF THE SCOUT RESEARCH VEHICLE

By Thomas C. Kelly

## SUMMARY

An investigation to determine the fin loads on a 1/8-scale model simulating the first stage of the Scout research vehicle was made in the Langley 8-foot transonic tunnel at Mach numbers from 0.40 to 1.20. Tests were conducted over an angle-of-attack range from about $-10^{\circ}$ to $10^{\circ}$ and at a Reynolds number per foot of approximately $3.5 \times 10^{6}$.

Results of the tests indicate that for a given angle of attack, negative tip-control deflections caused decreases in normal-force and fin-bending-moment coefficients and increases in pitching-moment coefficient, as would be expected. The effects were slight at a model angle of attack of $-10^{\circ}$ where tip-control stall had probably occurred but increased with an increase in angle of attack.

## INTRODUCTION

An investigation has been conducted in the Langley 8-foot transonic tunnel to determine the aerodynamic forces on the fin of a 1/8-scale model simulating the first stage of the Scout research vehicle. This investigation was required in order to obtain loads information on which to base the structural design of the fin. The effects on fin loads of the deflection of a control which formed the tip of the delta fin were determined. Reference 1 contains results obtained at a Mach number of 2.01 for the same model.

The results of the present investigation are presented for fin roll angles (from the vertical) of $0^{\circ}$, $45^{\circ}$, and $90^{\circ}$ and tip-control deflection angles of $0^{\circ}$, $-10^{\circ}$, and $-20^{\circ}$. Tests extended over a Mach number range from 0.40 to 1.20 and an angle-of-attack range from approximately $-10^{\circ}$ to $10^{\circ}$. Results are presented with only brief analysis in order to expedite publication.

## SYMBOLS

Aerodynamic force and moment data are referred to the body-axis system (fig. 1) with the moment reference center at the 67-percent-chord station of the fin root chord, which corresponds to the 50-percent-chord station of the mean geometric chord. (See fig. 2(a).)

$b$ span of exposed single fin, in.

$C_b$ fin-bending-moment coefficient, $\frac{M_b}{qSb}$

$C_{b_\alpha} = \frac{\partial C_b}{\partial \alpha}$, per degree

$C_m$ pitching-moment coefficient, $\frac{M_Y}{qS\bar{c}}$

$C_{m_\alpha} = \frac{\partial C_m}{\partial \alpha}$, per degree

$C_N$ normal-force coefficient, $\frac{F_N}{qS}$

$C_{N_\alpha} = \frac{\partial C_N}{\partial \alpha}$, per degree

$\bar{c}$ mean geometric chord of exposed fin, in.

$c_r$ root chord of exposed fin, in.

$F_N$ fin normal force

$M$ Mach number

$M_b$ bending moment about fin root

$M_Y$ pitching moment about $0.67c_r$ (or $0.50\bar{c}$)

$q$ free-stream dynamic pressure, lb/sq ft

$S$ fin area, exposed, sq ft

$x$ distance measured chordwise along $\bar{c}$ from fin leading edge, in.

| | |
|---|---|
| $y$ | distance measured spanwise from fin-body juncture, in. |
| $\alpha$ | angle of attack of body center line, deg |
| $\delta_t$ | tip-control deflection angle, positive when leading edge up and fin in horizontal plane ($\phi = 90^\circ$), deg |
| $\phi$ | fin roll angle, deg |

Subscript:

| | |
|---|---|
| cp | center of pressure |

## APPARATUS AND TESTS

### Model

Model details and design dimensions are given in figure 2(a). The cruciform fins, mounted with the trailing edge in line with the model base, had 45° sweepback of the leading edge and had single-wedge airfoil sections with rounded leading edges. The streamwise included wedge angle was 7.5° and the leading-edge radius, measured normal to the fin leading edge, was 0.031 inch. One fin was attached to an electrical strain-gage balance housed within the body and was free to move with respect to the body. The other three fins were rigidly attached. Although no attempt was made to seal the gap between the instrumented fin and the body, all other openings in the body were sealed to prevent air passage.

The instrumented fin was equipped with a tip control which could be manually set to the desired deflection angle. The tip-control hinge line was located at 63 percent of the tip-control root chord. (See fig. 2(b).)

Although the fin dimensions and the ratio of the fin span to the body diameter represent an actual 1/8-scale model of a proposed Scout configuration, limitations on model size made it necessary to reduce model length from that required for an actual 1/8-scale model. Photographs of the model are presented as figure 3.

### Tests and Procedure

Tests were conducted in the Langley 8-foot transonic tunnel and, for one fin orientation angle, in the Langley 8-foot transonic pressure tunnel at Mach numbers from about 0.40 to 1.20 and angles of attack from approximately -10° to 10°. Tests in the 8-foot transonic pressure tunnel

were required in order to overcome model fouling problems which occurred when the fin was in the horizontal position ($\phi = 90^\circ$) and the resultant fin loads were highest. Because the tests were made in different tunnels, some variation in Reynolds number occurred. These variations are shown in figure 4.

All tests were conducted with transition fixed at 10 percent of the local fin chord. For fin roll angles of $0^\circ$ and $45^\circ$, the transition strips were 0.1 inch wide and were composed of No. 120 carborundum grains set in a plastic adhesive. For the fin roll angle of $90^\circ$, similar strips employing No. 60 carborundum grains were used.



## Measurements

Aerodynamic forces and moments were determined by means of an electrical strain-gage balance housed within the body of the model. The balance was, in turn, rigidly fastened to a sting support.

Because of an inoperative component in the strain-gage balance, no axial-force results are included in the present paper.

## Corrections

Effects of subsonic boundary interference in the slotted test section are considered negligible and no corrections for these effects have been applied. At supersonic speeds the data are generally affected by boundary-reflected disturbances which, for the present model, were estimated to occur between Mach numbers of about 1.10 and 1.20. Schlieren photographs, presented in figure 5, show the flow over the fin to be free of reflected disturbances except at a Mach number of 1.20 and an angle of attack of $10^\circ$ where some relatively weak reflected disturbances may be noted. The effects of these disturbances are unknown; however, results for a Mach number of 1.20 are included to allow comparison with results obtained at higher speeds.

Angles of attack and roll have not been corrected for deflection of the balance and sting under load. However, static loadings equivalent to the measured air loads were made subsequent to the tests and indicated that maximum deflections (which were experienced at a Mach number of 1.20 and an angle of attack at $10^\circ$) did not exceed $0.16^\circ$ in pitch and $1.21^\circ$ in roll. It is felt that these deflections would not significantly affect the results presented herein.

## PRESENTATION OF RESULTS

In order to facilitate presentation of the data, staggered scales have been used in some of the figures and care should be taken in selecting the proper zero axis for each curve. The figures presenting results of this investigation are as follows:



## DISCUSSION

### Effects of Fin Roll and Tip-Control Deflection

The effects on the various aerodynamic characteristics of varying the fin roll angle from $0^\circ$ to $90^\circ$ may be seen by comparing figures 6 to 8. The results show expected variations. The effects of tip-control deflection, shown in figures 6 to 8, also indicate expected variations in that as control deflections are increased in the negative direction reductions in normal-force coefficient occur at a given angle of attack, along with increases in pitching-moment coefficient and reductions in fin-bending-moment coefficient. The effects noted are slight at a model angle of attack of $-10^\circ$ where the tip control is operating at an angle of attack of $-20^\circ$ or $-30^\circ$ (depending upon $\delta_t$) and tip stall has occurred. Increases in model angle of attack are accompanied by increases in tip-control effectiveness, as would be expected, over the angle-of-attack range of these tests.

### Effects of Mach Number

The effects of increasing Mach number are summarized in figure 10 for a fin roll angle $\phi$ of $90^\circ$. These results are for a tip-control

deflection angle of 0° and a model angle of attack of 0°. Chordwise and spanwise centers of pressure were obtained using the slopes $C_{N_\alpha}$, $C_{m_\alpha}$, and $C_{b_\alpha}$ taken at an angle of attack of 0°. It should be noted that the chordwise centers of pressure are referred to the fin mean geometric chord, rather than the fin root chord. Shown for comparison are results obtained at a Mach number of 2.01 from reference 1. The results indicate that variations of normal-force, pitching-moment, and center-of-pressure characteristics with Mach number follow generally expected trends.



## CONCLUDING REMARKS

Results have been presented of an investigation to determine the fin loads on a 1/8-scale model simulating the first stage of the Scout research vehicle at Mach numbers from 0.40 to 1.20 and over an angle-of-attack range from about -10° to 10°. These results indicate that for a given angle of attack, negative tip-control deflections caused decreases in normal-force and fin-bending-moment coefficients and increases in pitching-moment coefficient, as would be expected. The effects were slight at a model angle of attack of -10° where tip-control stall had probably occurred but increased with an increase in angle of attack.

Langley Research Center,
National Aeronautics and Space Administration,
Langley Field, Va., April 27, 1961.

## REFERENCE

1. Robinson, Ross B., and Landrum, Emma Jean: Fin Loads and Tip-Control Hinge Moments on a 1/8-Scale Model Simulating the First Stage of the Scout Research Vehicle at a Mach Number of 2.01. NASA TM X-239, 1960.

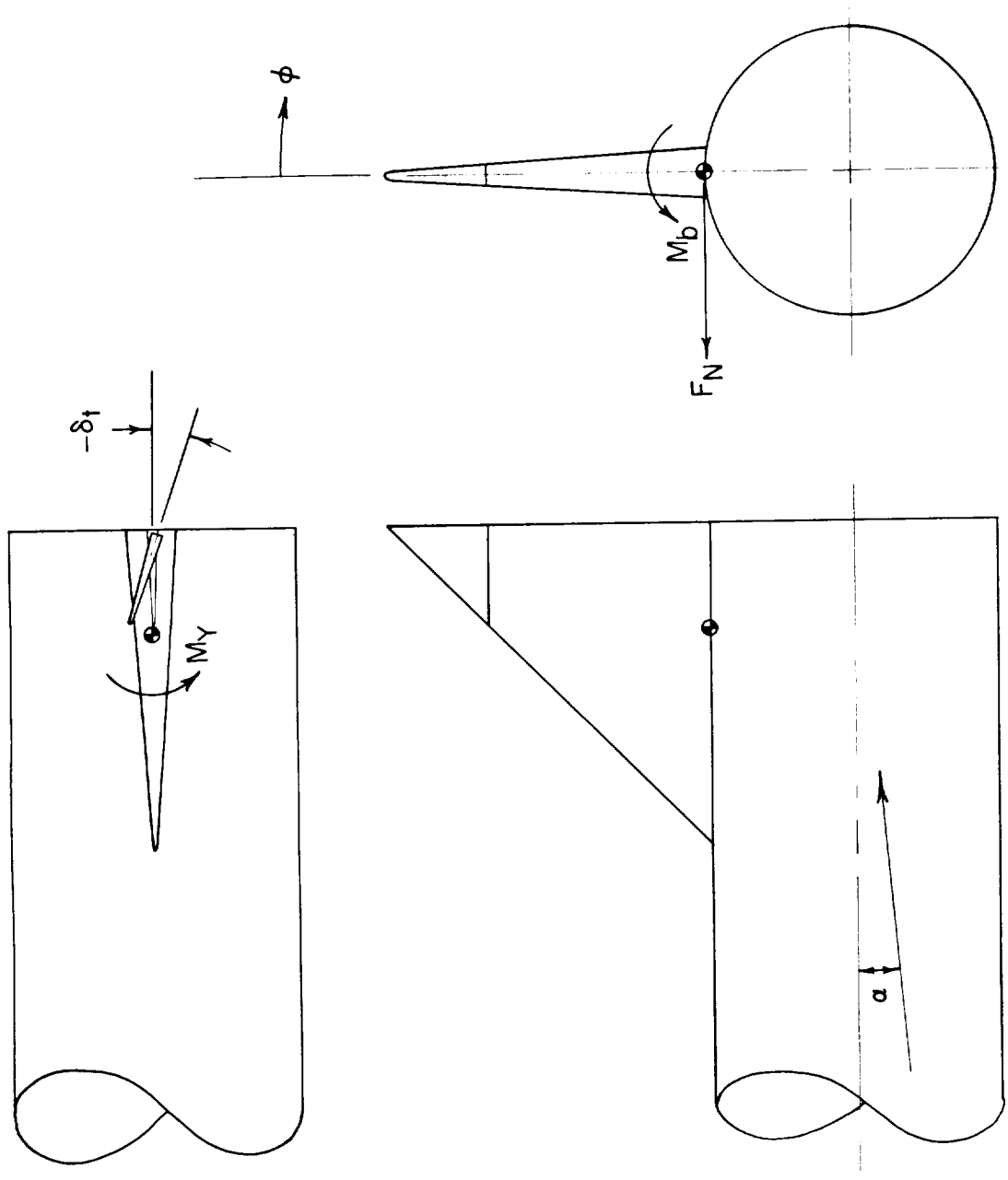


Figure 1.- Model axis system. Arrows indicate positive directions except as noted.

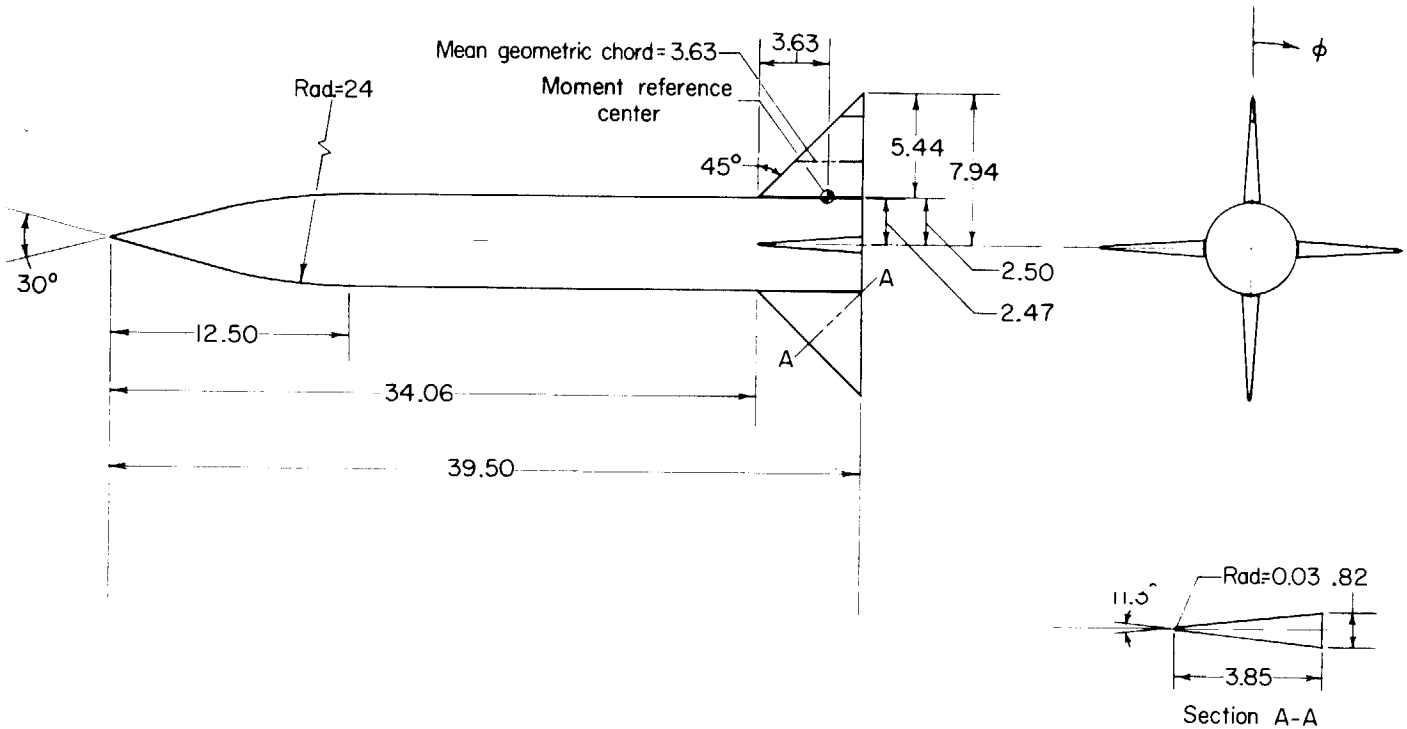


(a) Complete model.

Figure 2.- Model details. All dimensions in inches unless otherwise noted.

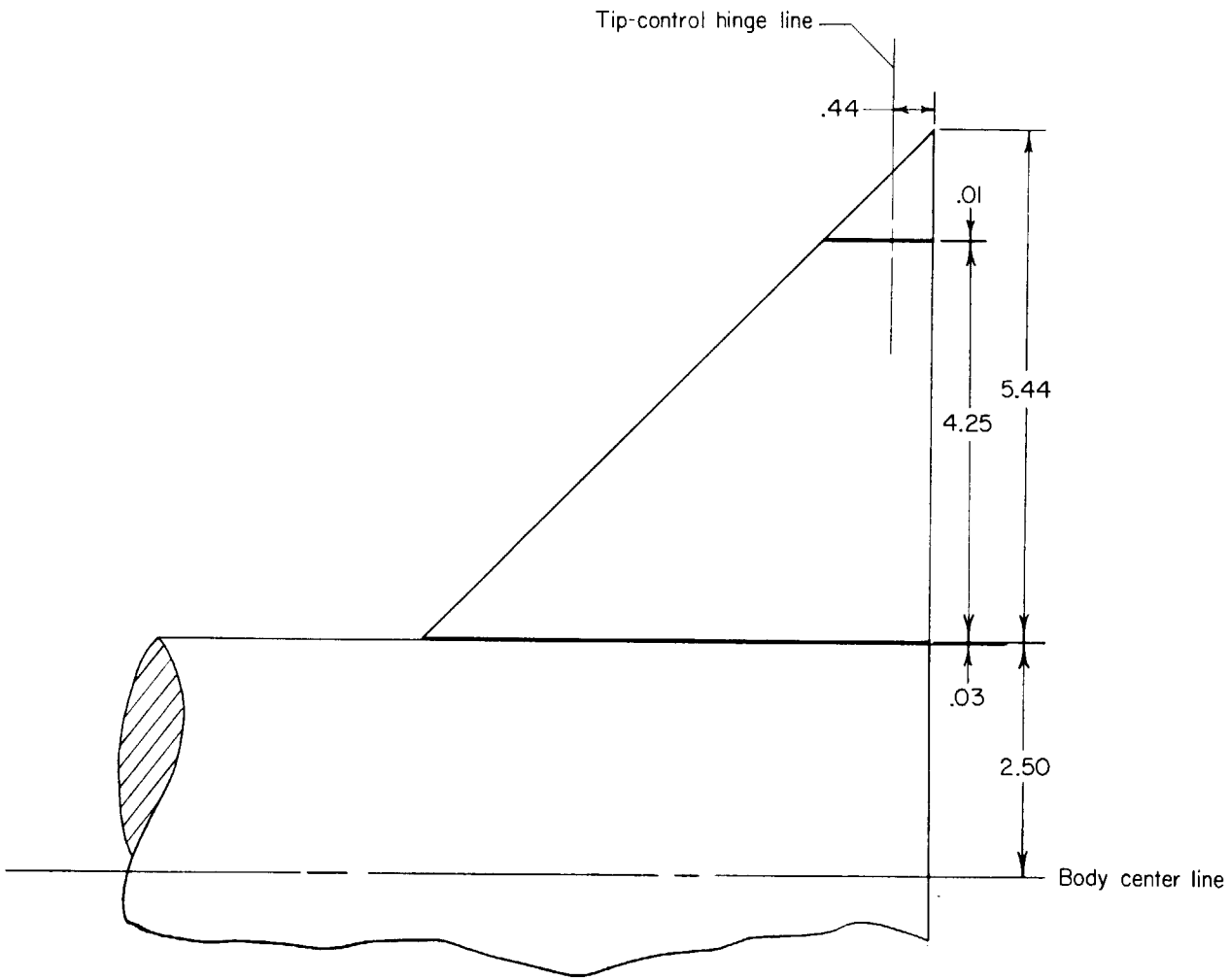


(b) Instrumented fin.

Figure 2.- Concluded.

(a) Three-quarter front view. L-59-2701

Figure 3.- Model photographs.

(b) Three-quarter rear view. L-59-2700

Figure 3.- Concluded.

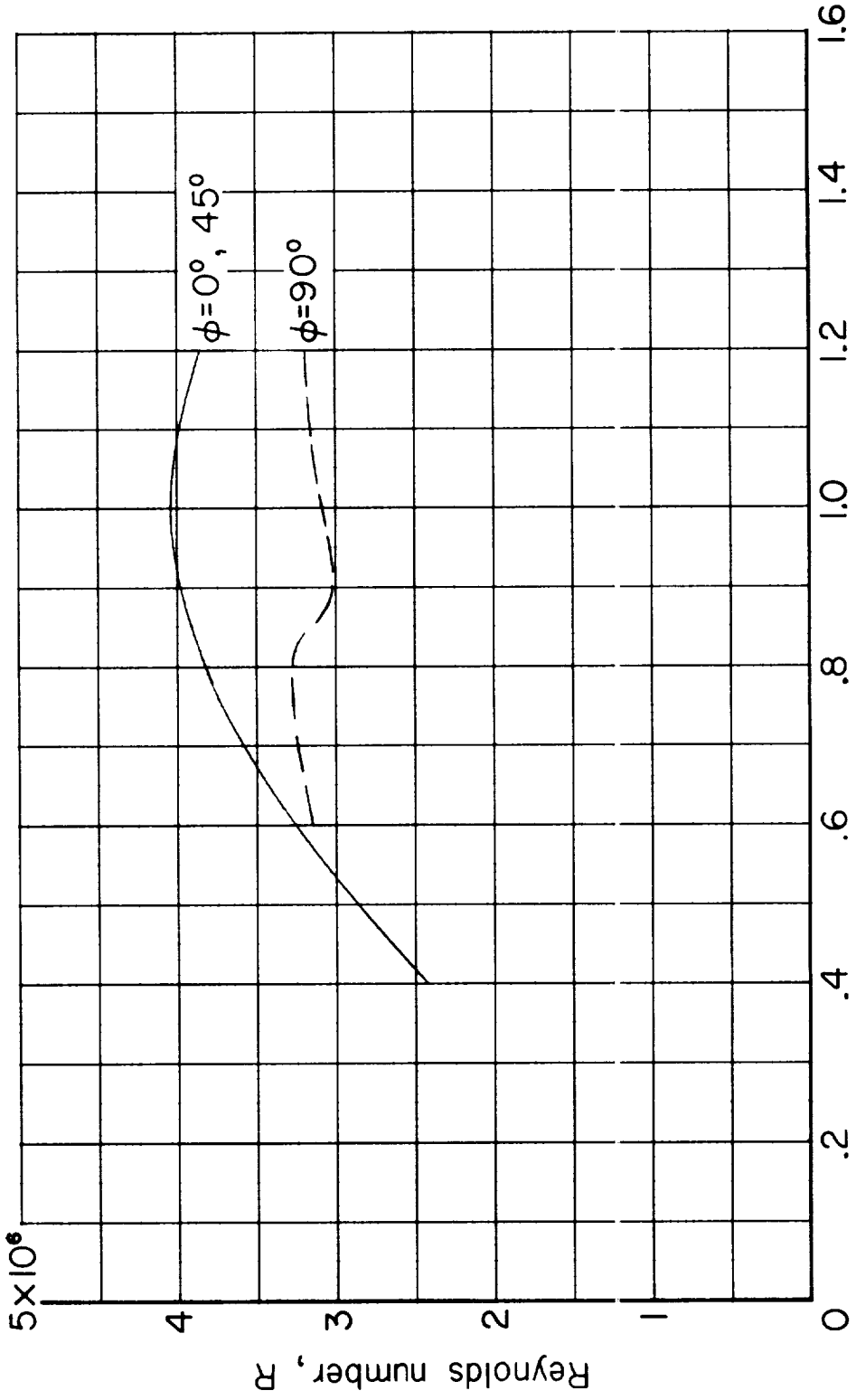


Figure 4.- Variation of average test Reynolds number per foot with Mach number.

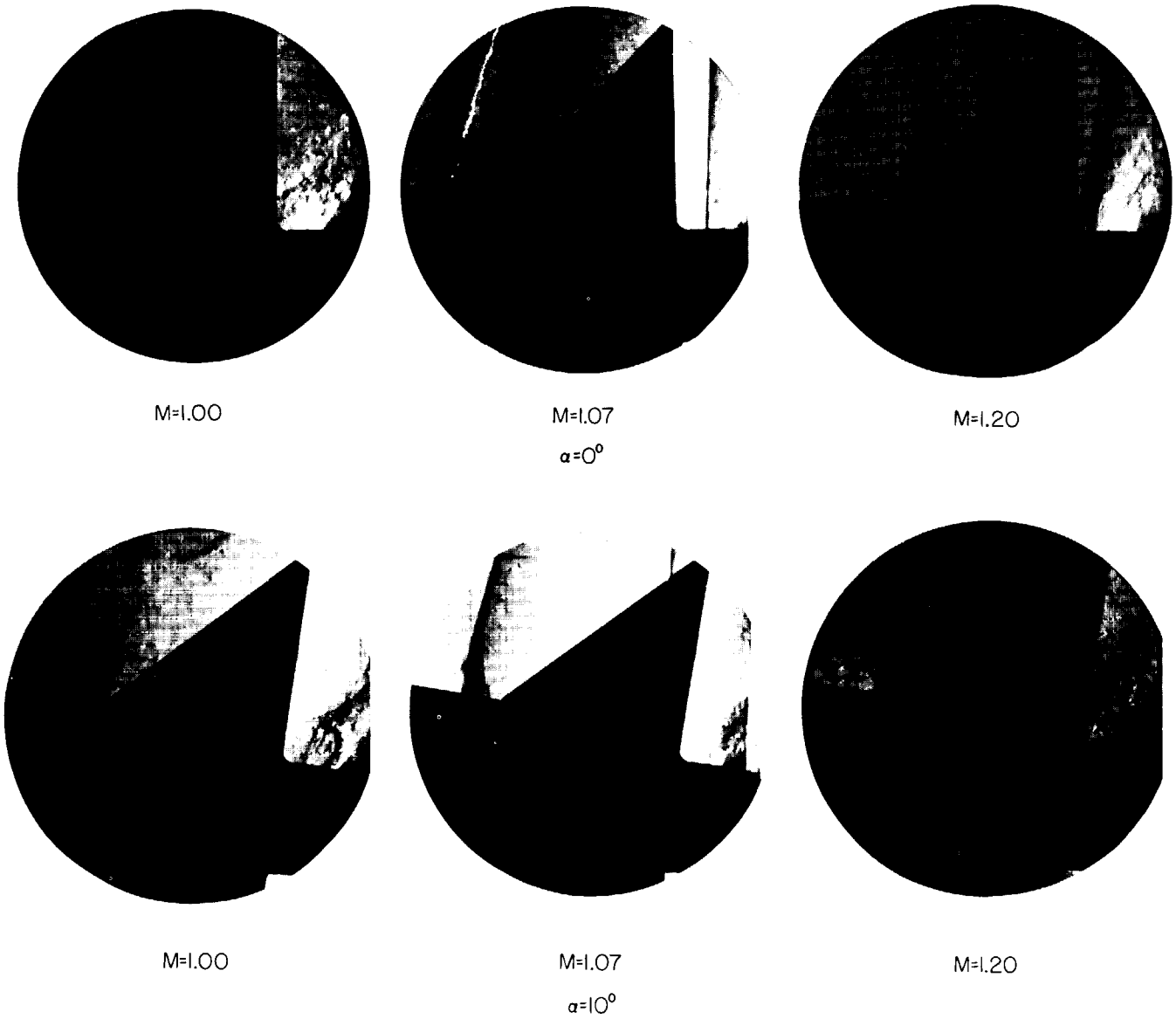


Figure 5.- Schlieren photographs of model fin. L-61-2159

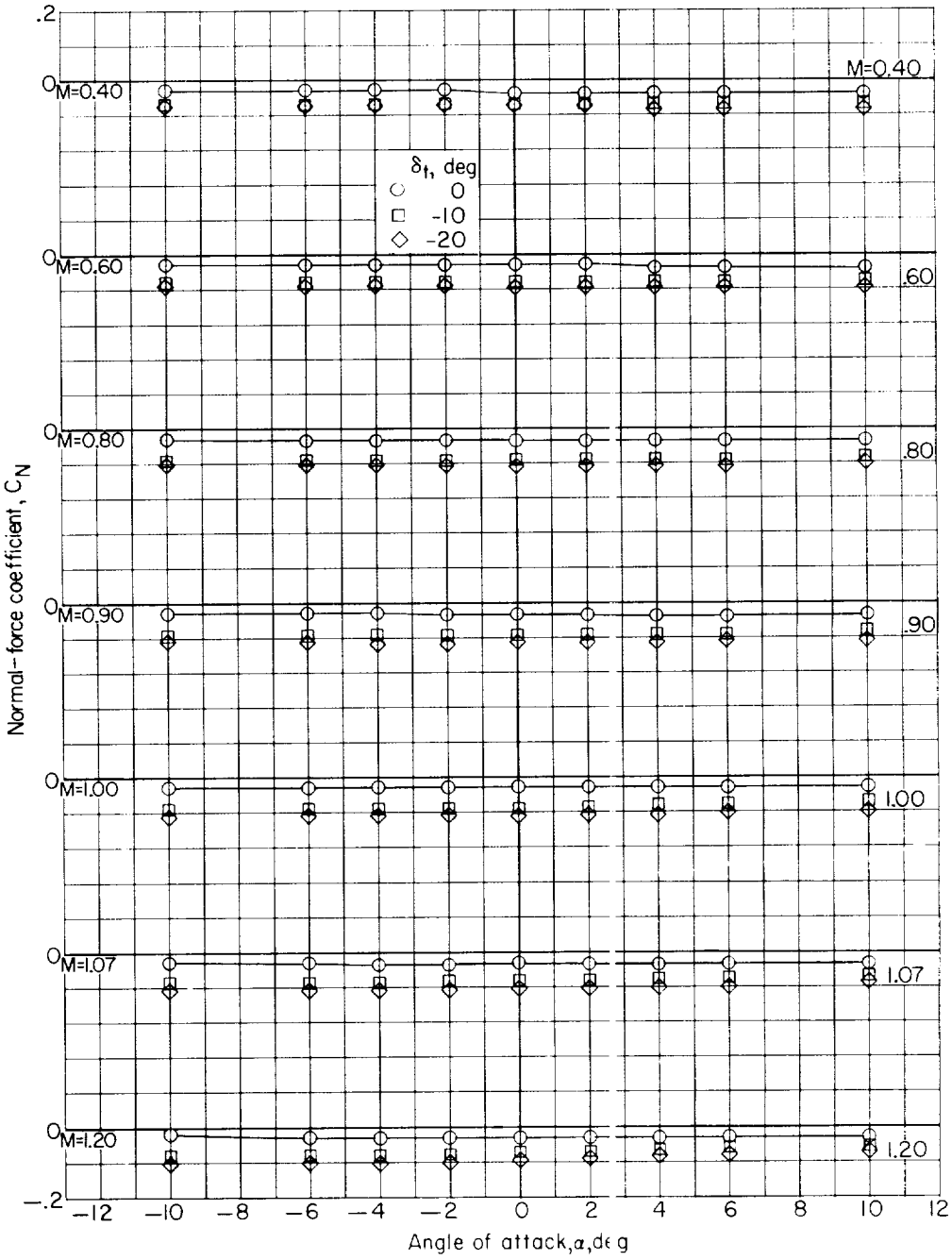


(a) $\phi = 0^{\circ}$.

Figure 6.- Effect of tip-control deflection on normal-force characteristics.

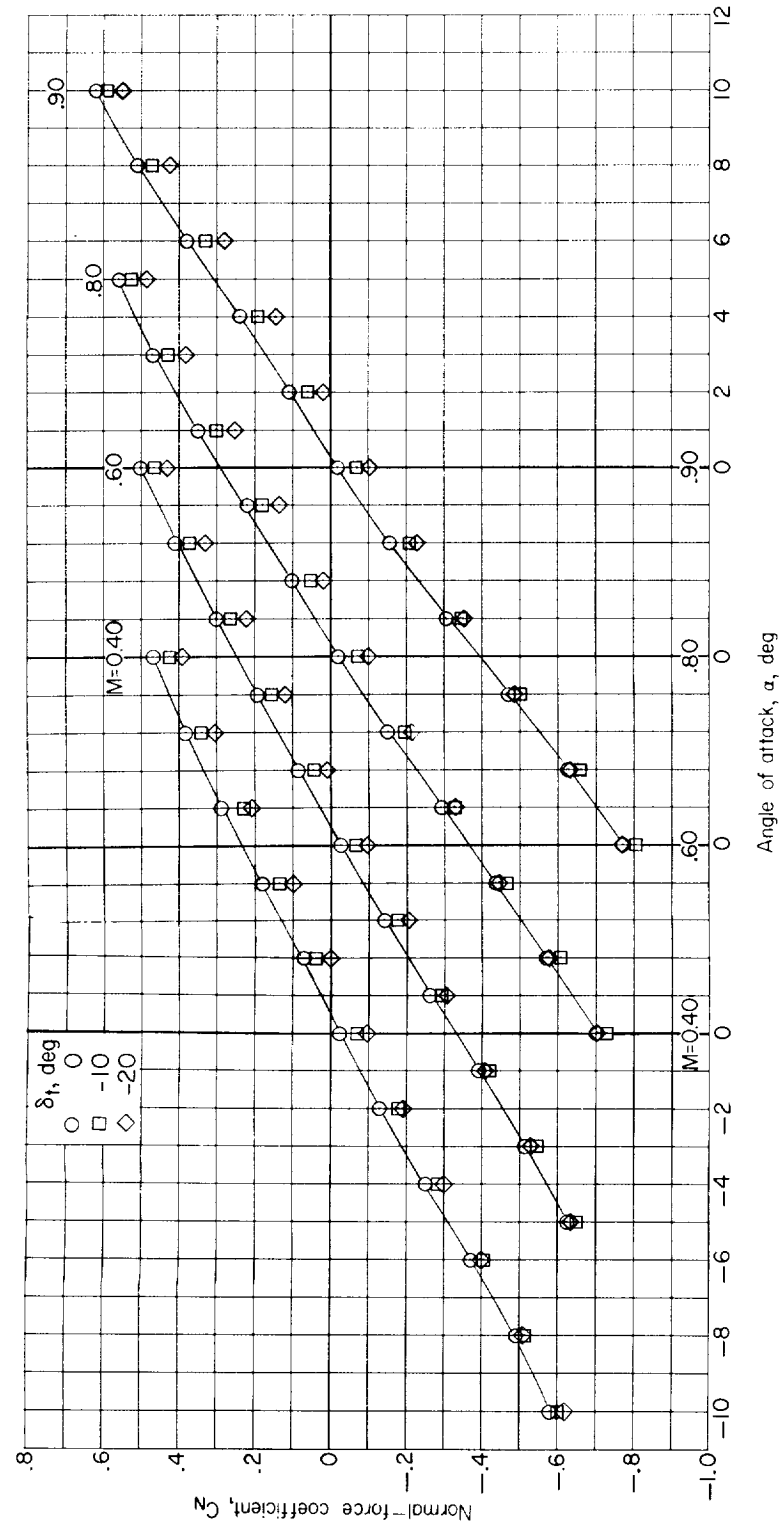


(b) $\phi = 45^\circ$.

Figure 6.- Continued.

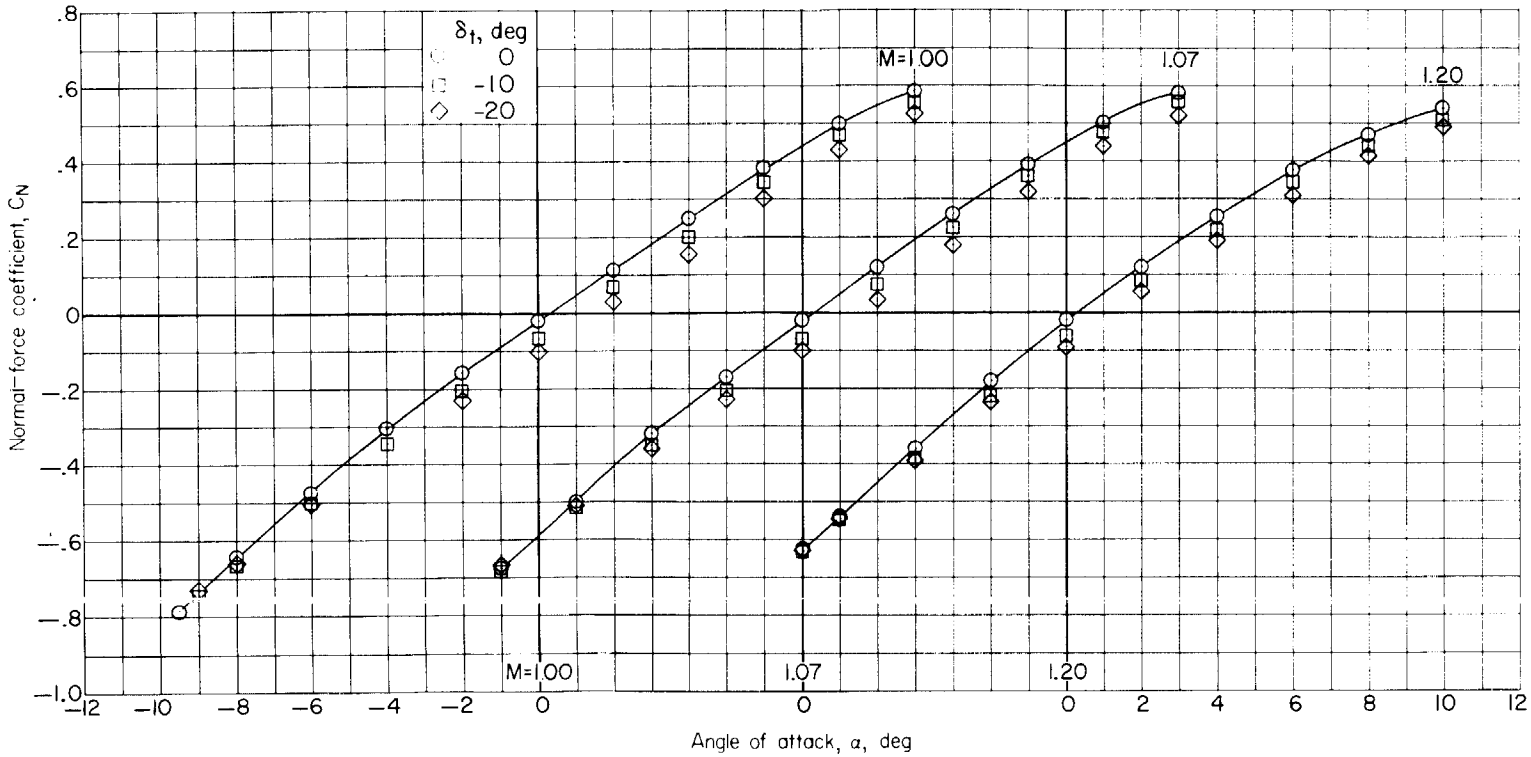


(b) Concluded.

Figure 6.- Continued.

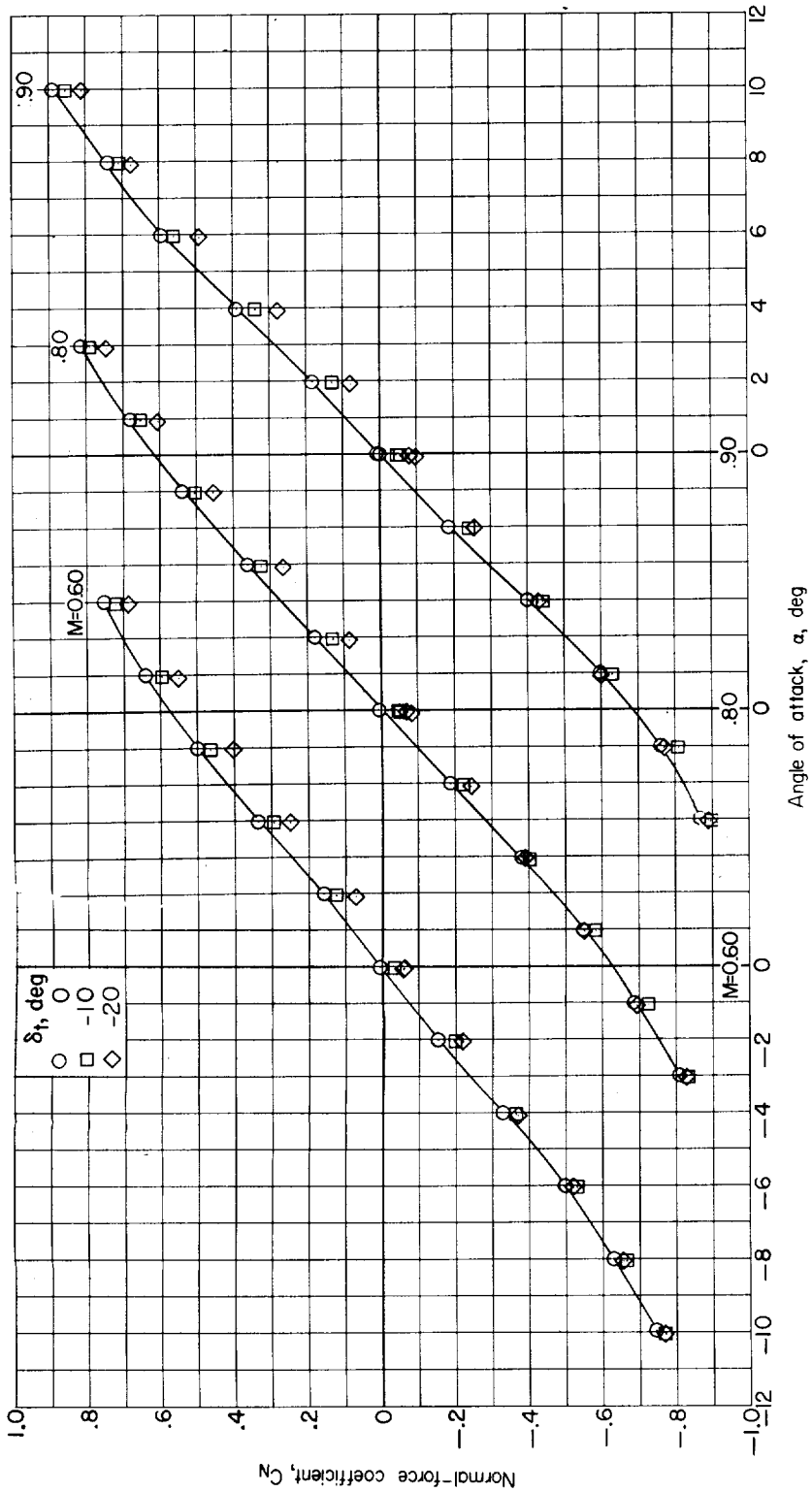


(c) $\phi = 90^\circ$.

Figure 6.- Continued.

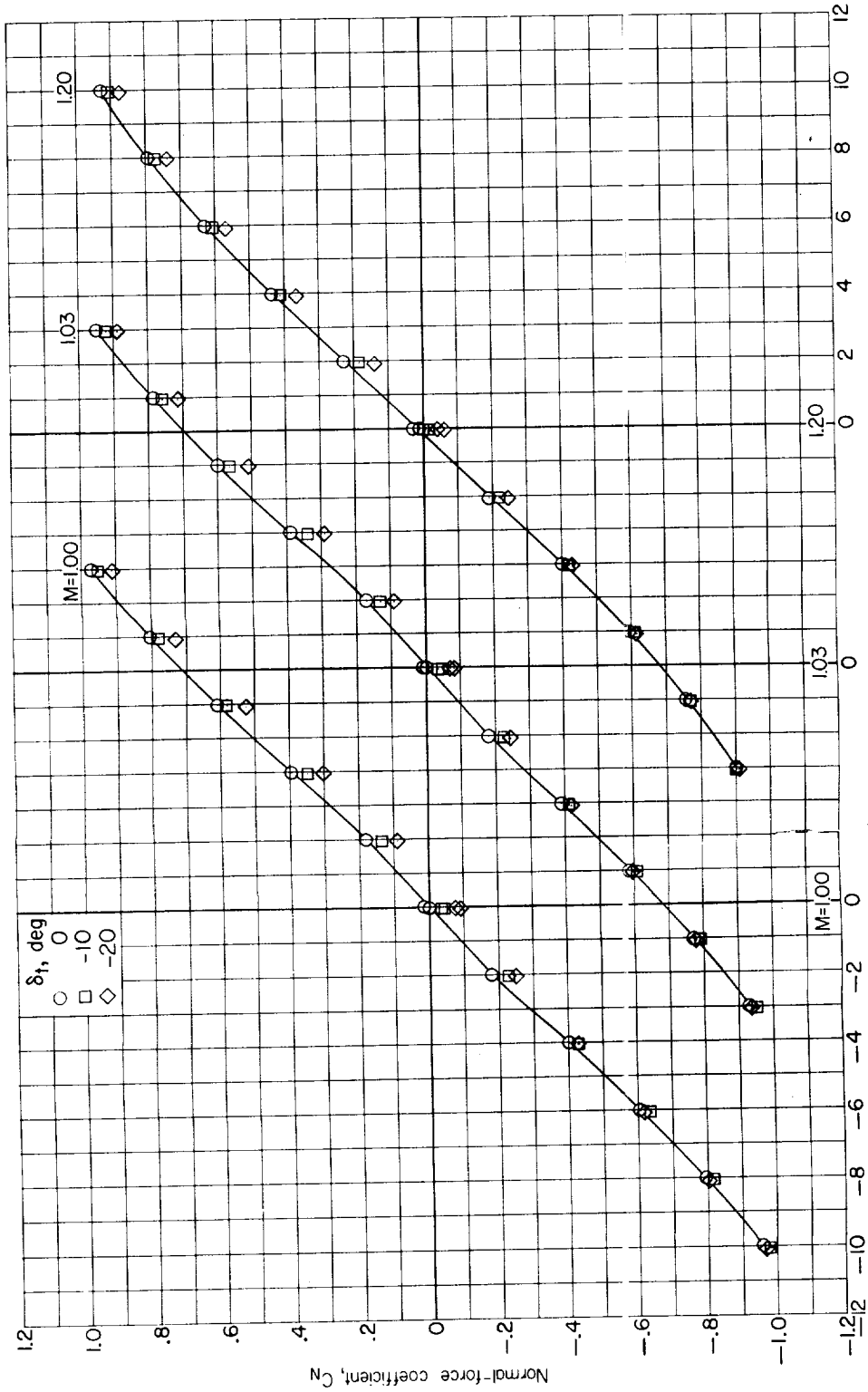


(c) Concluded.

Figure 6.- Concluded.

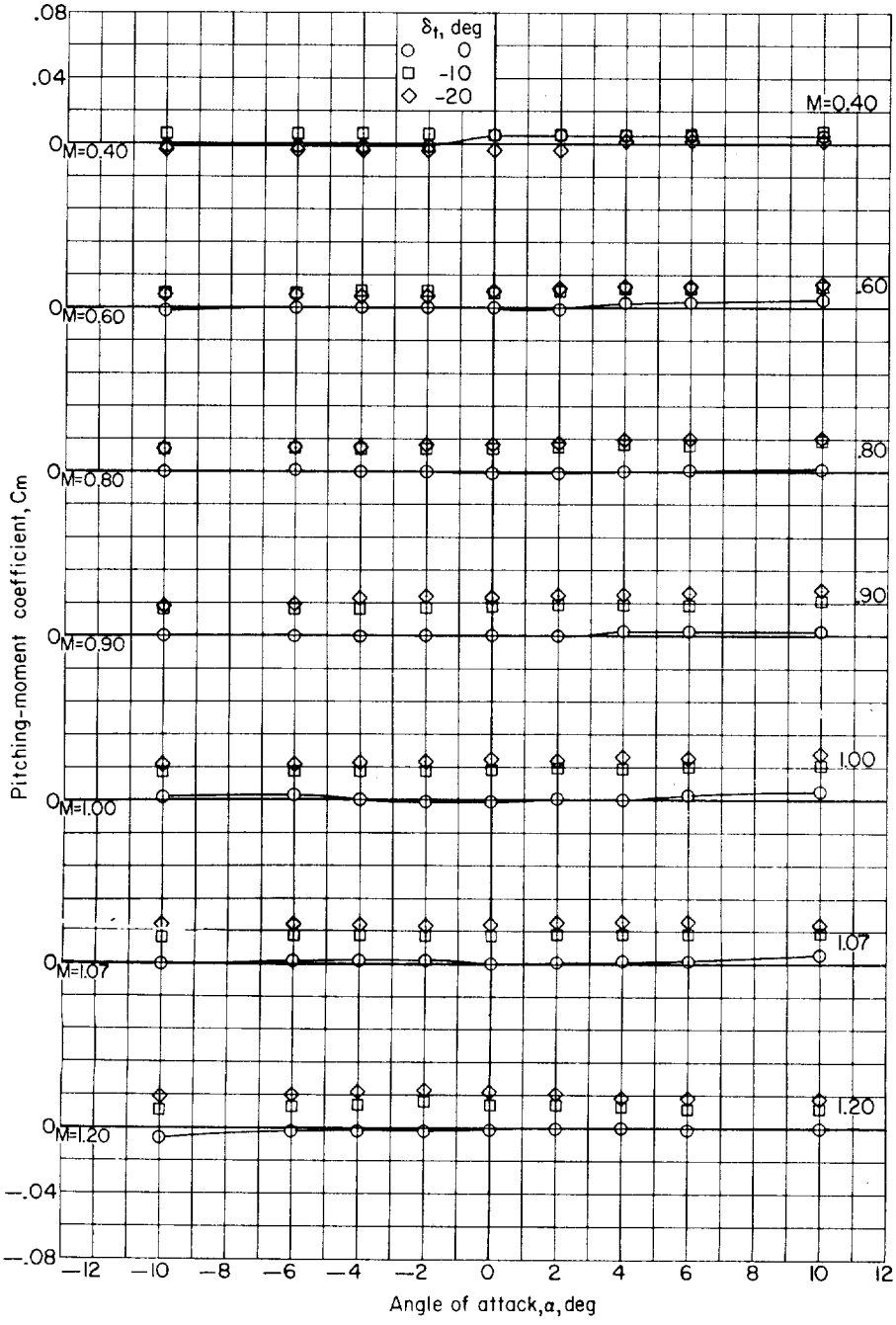


(a) $\phi = 0^{\circ}$.

Figure 7.- Effect of tip-control deflection on pitching-moment characteristics.

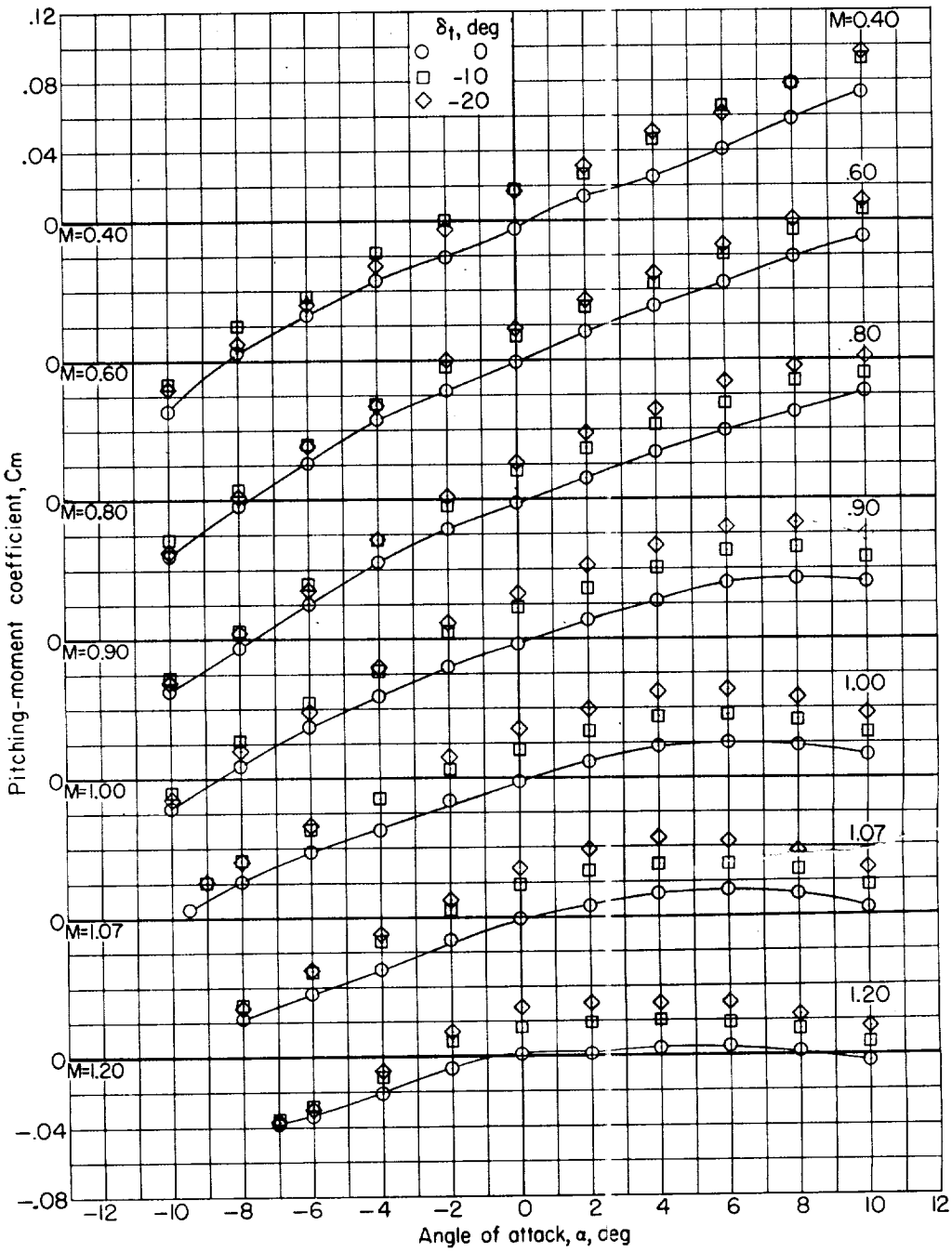


(b) $\phi = 45^\circ$.

Figure 7.- Continued.

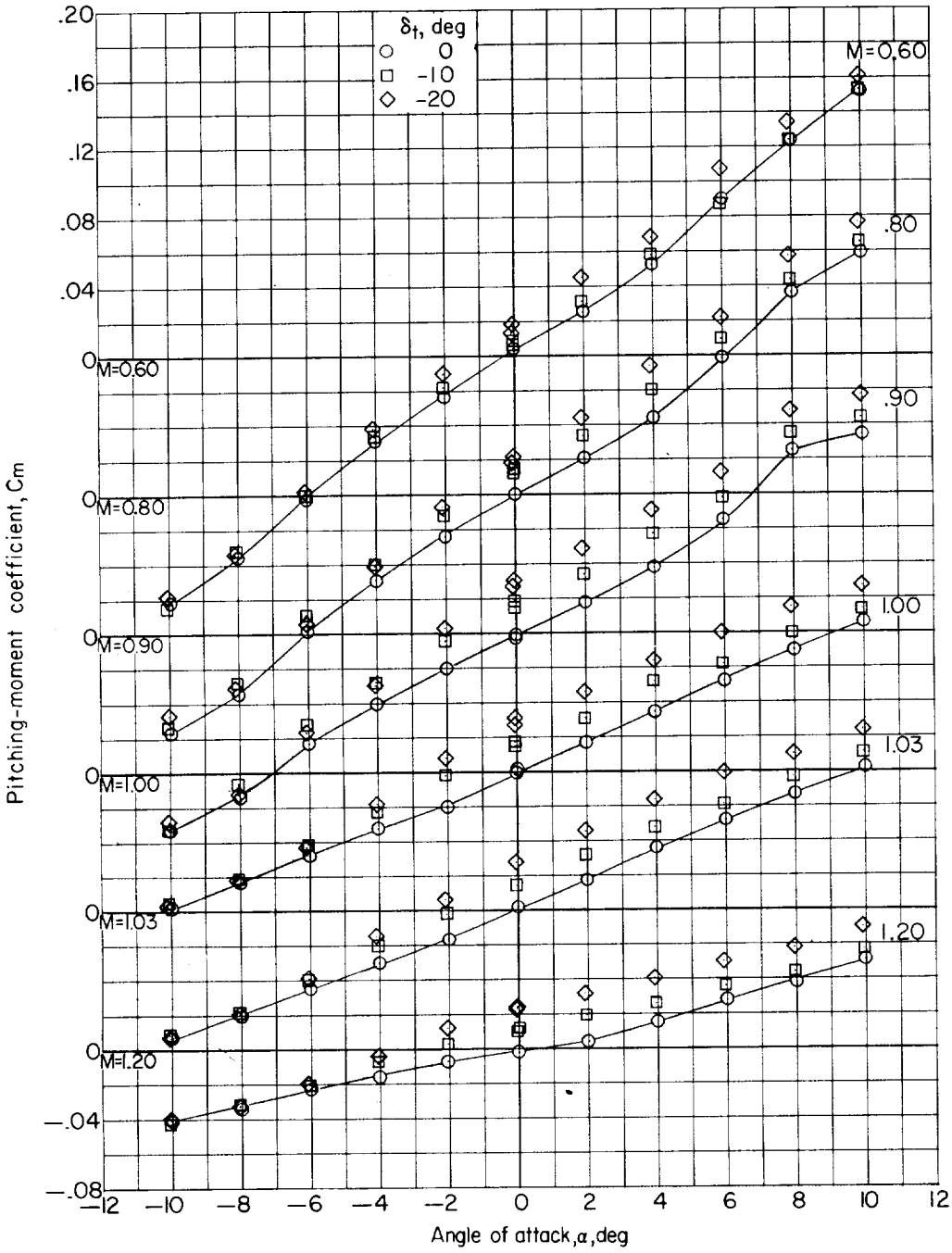


(c) $\phi = 90^\circ$.

Figure 7.- Concluded.

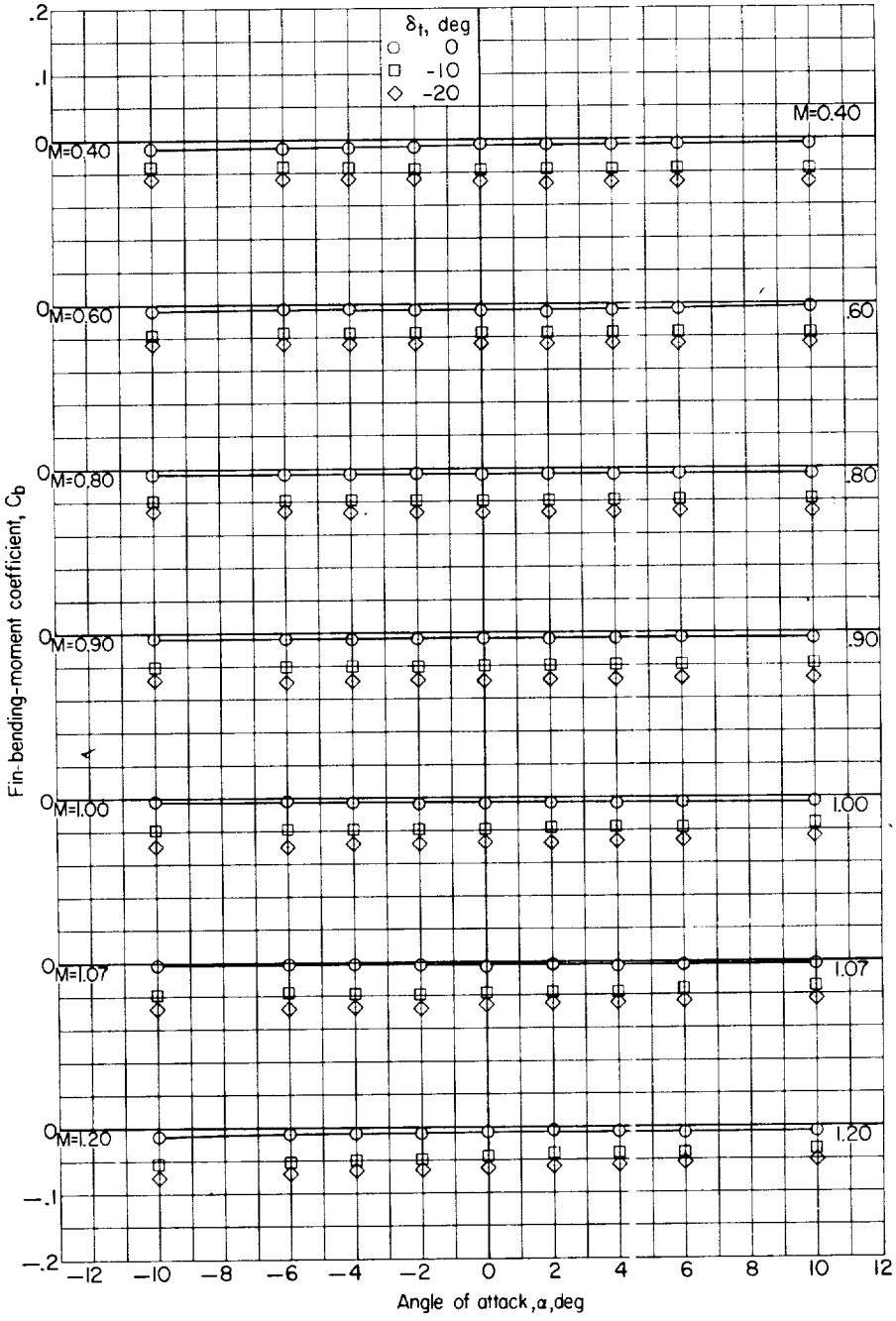


(a) $\phi = 0^\circ$.

Figure 8.- Effect of tip-control deflection on fin-bending-moment characteristics.

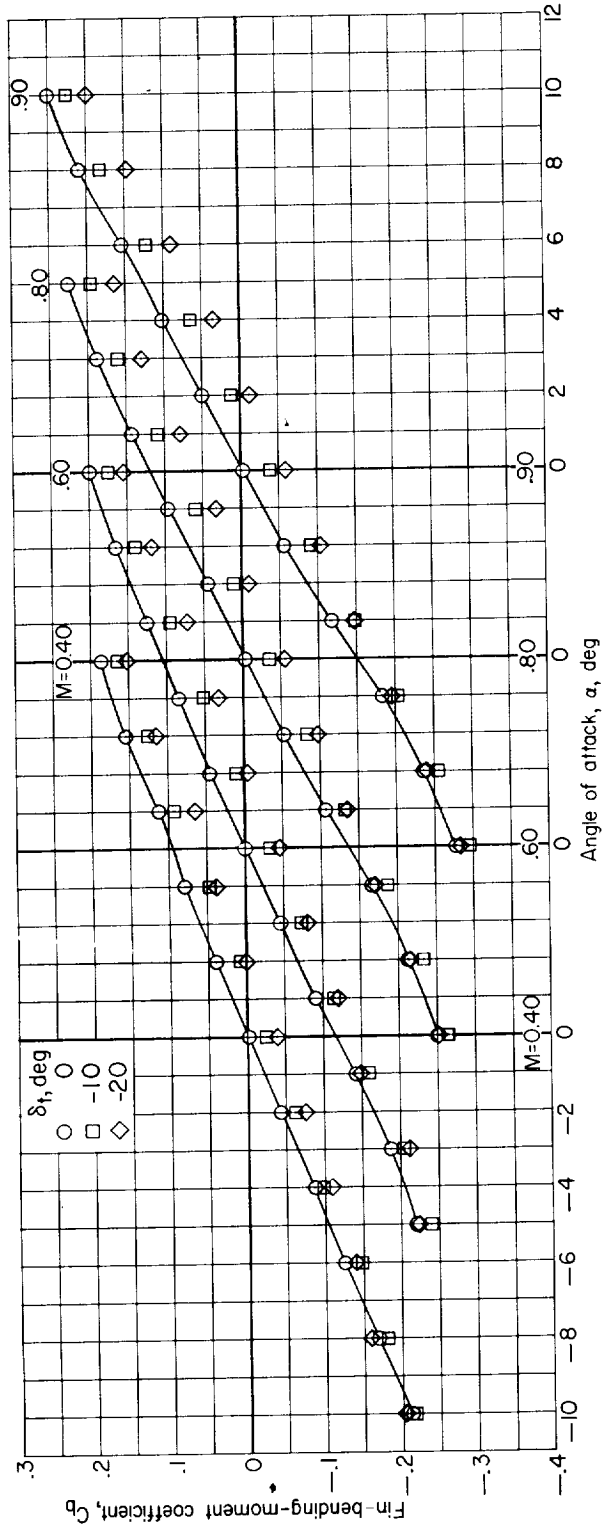


(b) $\phi = 45^\circ$.

Figure 8.- Continued.

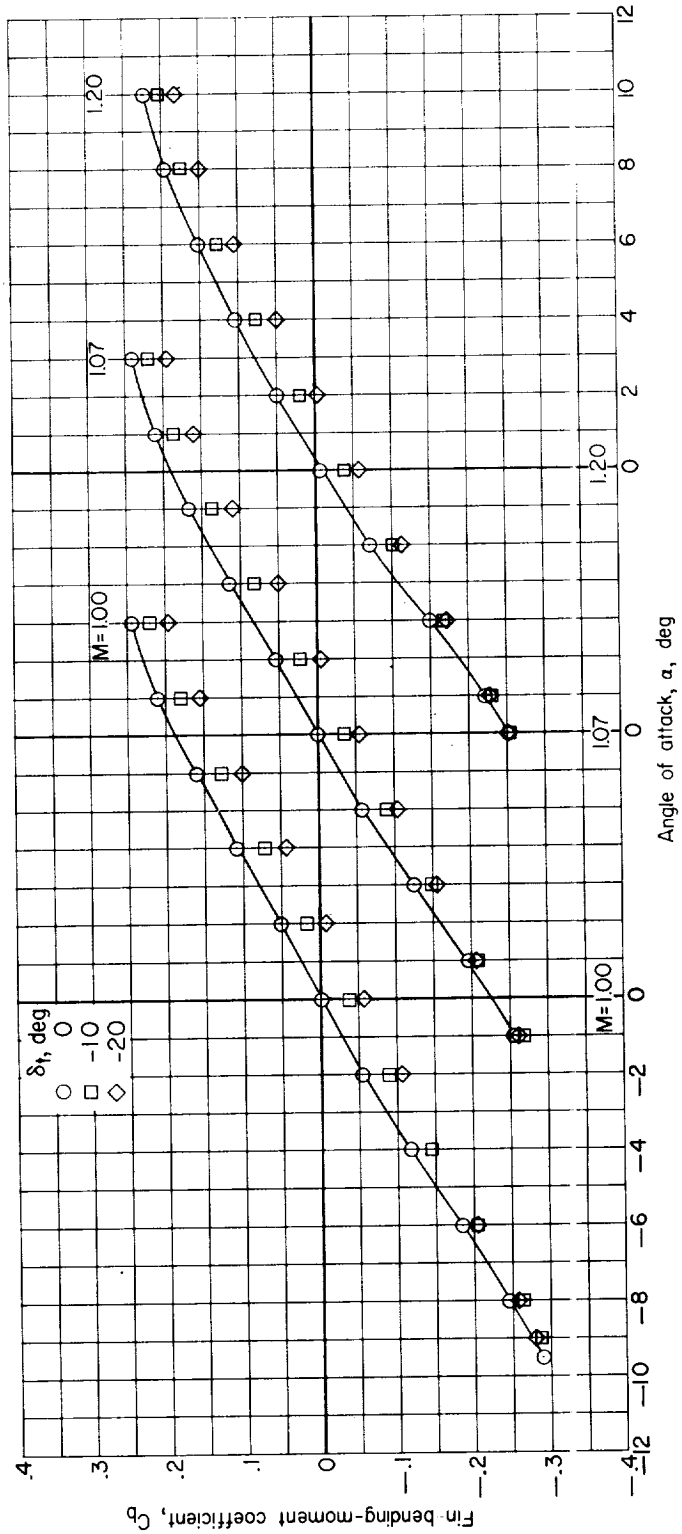


(b) Concluded.

Figure 8.- Continued.

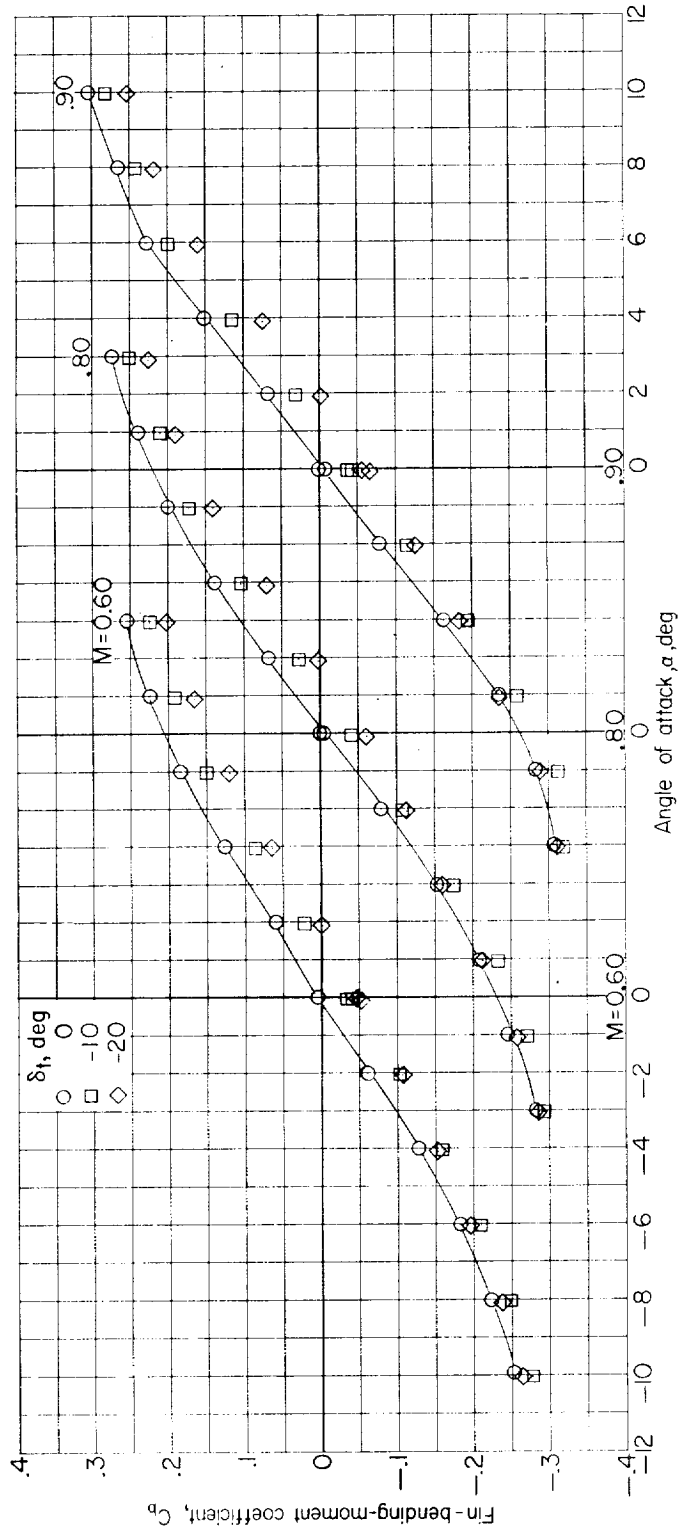


(c) $\phi = 90^\circ$.

Figure 8.- Continued.

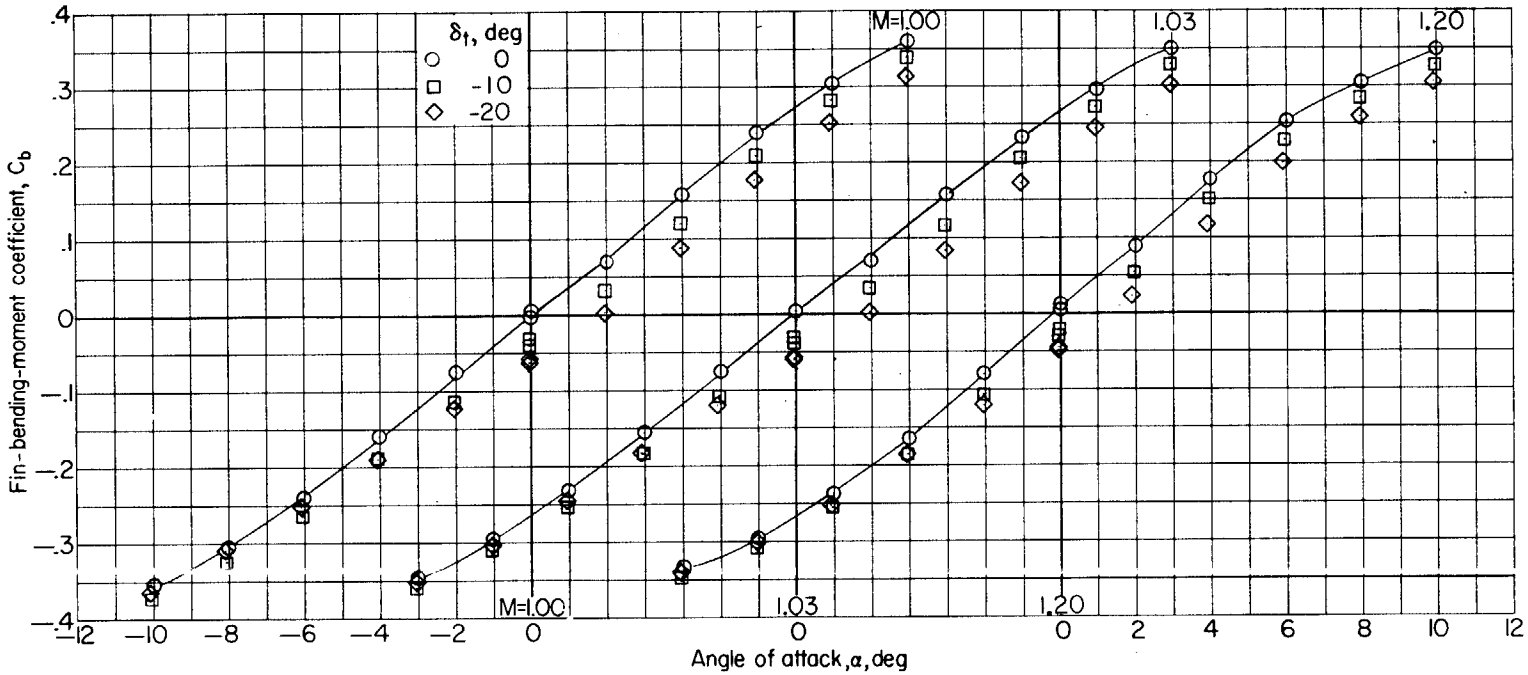


(c) Concluded.

Figure 8.- Concluded.

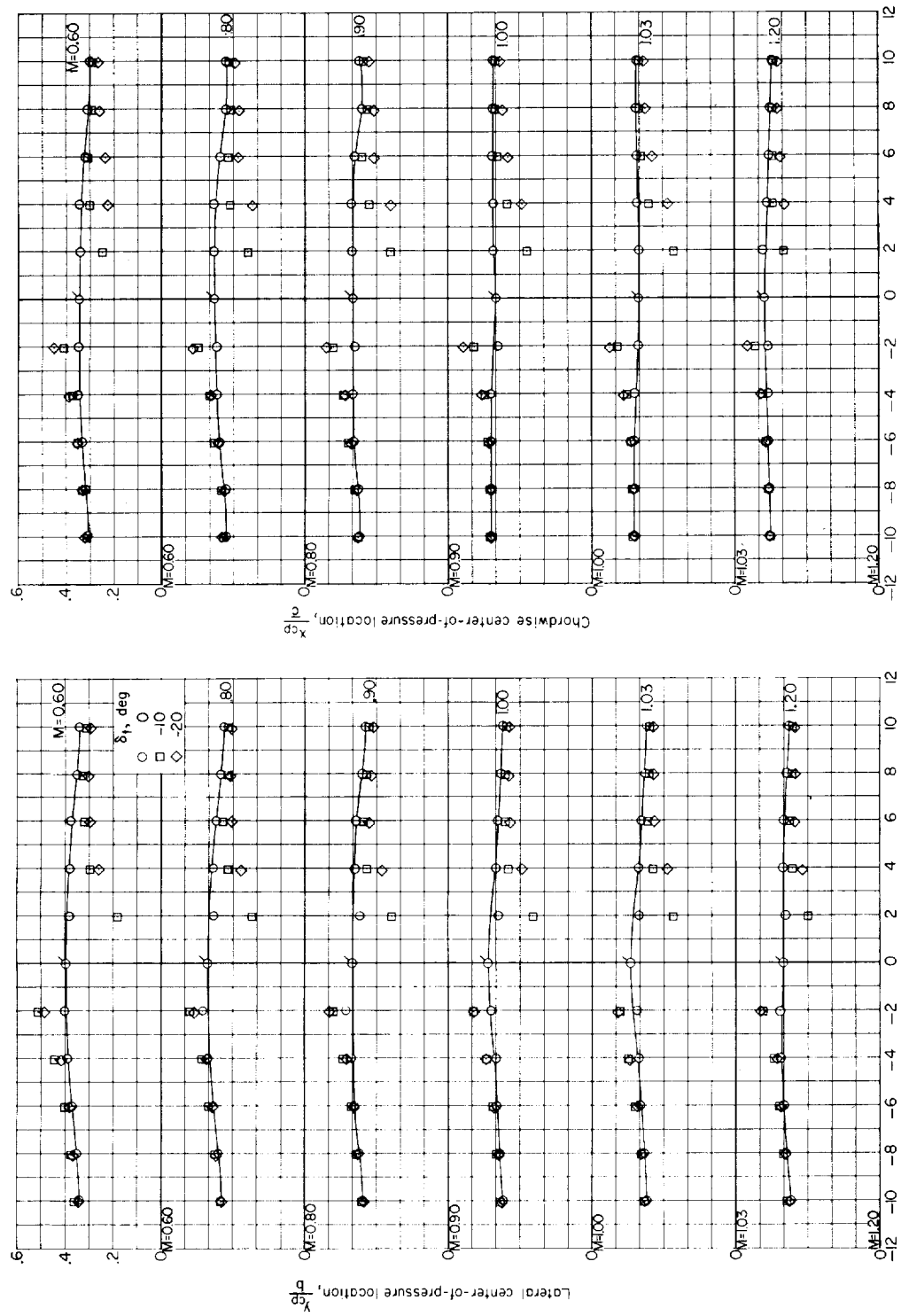


Figure 9.- Effect of tip-control deflection on center-of-pressure characteristics. $\phi = 90^{\circ}$. Flagged symbols indicate computed points.

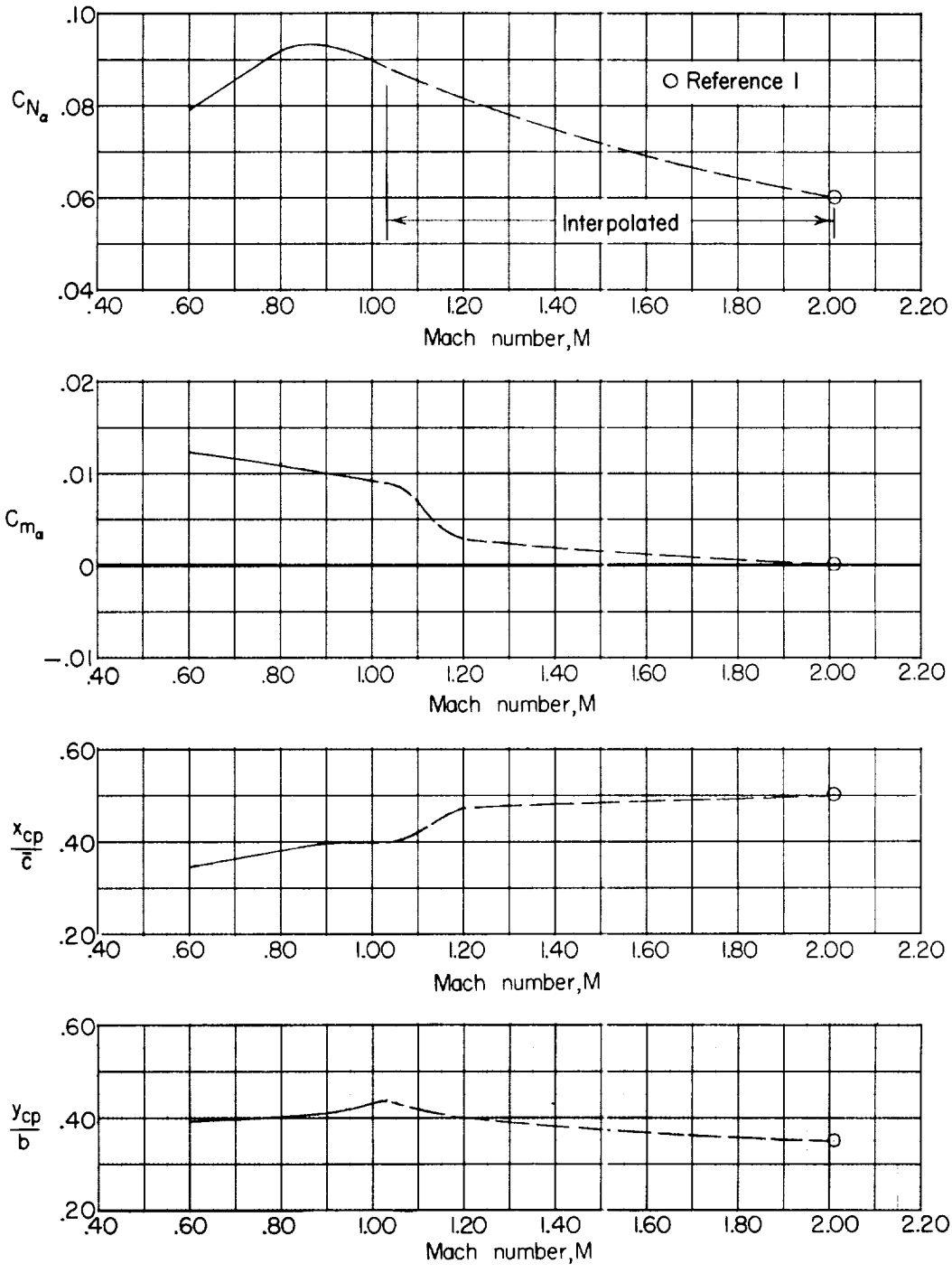


Figure 10.- Summary of aerodynamic characteristics.
$\phi = 90^\circ$; $\delta_t = 0^\circ$; $\alpha = 0^\circ$.



L-1438